Global and Planetary Change 98–99 (2012) 54–62

Contents lists available at SciVerse ScienceDirect

Global and Planetary Change

journal homepage: www.elsevier.com/locate/gloplacha

Positive precipitation–evaporation budget from AD 460 to 1090 in the Saloum Delta (Senegal) indicated by mollusk oxygen isotopes

Moufok Azzoug [a,*], Matthieu Carré [a], Brian M. Chase [a,g], Abdoulaye Deme [b], Alban Lazar [b,c], Claire E. Lazareth [c], Andrew J. Schauer [d], Magloire Mandeng-Yogo [c], Monique Simier [f], Amadou Thierno-Gaye [b], Luis Tito de Morais [e]

[a] UM2-CNRS-IRD, Institut des Sciences de l'Evolution de Montpellier, Université Montpellier 2, CC061, Pl. Eugène Bataillon, 34095 Montpellier, France
[b] Laboratoire de Physique de l'Atmosphère et de l'Océan Simeon Fongang, Université Cheikh Anta Diop, Dakar, Senegal
[c] IPSL/LOCEAN, UPMC/CNRS/IRD/MNHN, LOCEAN-IPSL, Center IRD France Nord, 32 avenue Henri Varagnat, 93143 Bondy CEDEX, France
[d] Department of Earth and Space Sciences, University of Washington, Seattle, WA, 98195, United States
[e] Laboratoire des Sciences de l'Environnement Marin, Université de Bretagne occidentale, BP 70, 29280, Plouzané, France
[f] IRD, UMR EME Ifremer-IRD-UM2, Centre de Recherche Halieutique Méditerranéenne et Tropicale, Avenue Jean Monnet, BP 171, 34203 Sète Cédex, France
[g] Department of Archaeology, History, Culture and Religion, University of Bergen, P.O. 7805, 5020, Bergen, Norway

ARTICLE INFO

Article history:
Received 21 May 2012
Accepted 14 August 2012
Available online 19 August 2012

Keywords:
West African Monsoon
mollusks
Saloum estuary
stable isotopes

ABSTRACT

There is a critical need to document the long-term variability of the West African Monsoon (WAM) in the Sahel region. We present here a multidecadal proxy record of the past hydrology from AD 460 to 1090 in the Saloum Delta, Senegal. The Saloum Delta is a hypersaline estuary where the salinity and the water isotopic composition are highly sensitive to rainfall variations. The past hydrology was studied using the oxygen isotopic ratio of *Anadara senilis* fossil shells, since mollusk shell isotopic composition ($\delta^{18}O$) in this environment is primarily determined by the precipitation–evaporation budget. Successive samples of shells were taken along the stratigraphy of the massive Dioron Boumak fossil shell middens for new insights into the past WAM multi-decadal to centennial variability. The averaged $\delta^{18}O$ value of fossil shells was more negative by 1.4‰ compared to modern shells' isotopic signature. This result indicates substantially fresher mean conditions in the Saloum Delta, that was likely not hypersaline as it is today. The precipitation–evaporation budget was thus more positive in response to a more intense and/or longer monsoon season during the studied period. Our record suggests that strong multidecadal droughts as observed in the Sahel in the late 20th century did likely not occur in Senegal during this ~600-yr time period.

1. Introduction

The West African Monsoon (WAM) is an important component of the global climate system and is related to the seasonal latitudinal displacement of the Intertropical Convergence Zone (ITCZ). Precipitation brought by the WAM plays a critical socio-economical role in the countries of the Sahel region, whose economies are considered to be particularly vulnerable to climate change (Sultan et al., 2005). From the 1960s to the 2000s, the Sahel experienced a 30–40% precipitation drop off (Hulme, 2001; Nicholson and Grist, 2003) which represents the most significant multi-decadal climate signal of the 20th century (Dai et al., 2004a, 2004b; IPCC, 2007) and had a devastating impact on regional populations (Myers, 2002; Davidson et al., 2003; Stige et al., 2006). These issues have made the study of WAM dynamics on infra-seasonal to millennial time scales an important focus of the scientific community.

Based on instrumental records, a multi-decadal modulation of the Sahel precipitation has been identified, likely related to the Atlantic Multi-decadal Oscillation (AMO) (Folland et al., 1986; Nicholson, 2000; Zhang and Delworth, 2006). Additional significant factors affecting WAM activity include variations in tropical sea-surface temperatures (SSTs) (Giannini et al., 2003), El Niño Southern Oscillation (ENSO) (Janicot et al., 2001), continental convection processes (Lebel et al., 2003), land use and albedo feedbacks (Charney, 1975). In spite of these significant advances, the understanding of the WAM variability on multi-decadal to centennial timescales is still limited by the restricted length of instrumental records, which needs consequently to be extended by paleoclimatic proxy records.

This study is focused on climatic conditions in Senegal from ~AD 460 to 1090, a period that corresponds roughly to the Dark Age Cold Period (DACP) and the beginning of the Medieval Warm Period (MWP) identified in Europe (Mcdermott et al., 2005; Mann et al., 2009; Ljungqvist, 2010; Wanner et al., 2011). Evidence for paleohydrological change in tropical Africa during this period has been recognized in several locations. Lake level reconstructions show that this period was characterized

* Corresponding author.
E-mail address: moufok.azzoug@univ-montp2.fr (M. Azzoug).

0921-8181/$ – see front matter © 2012 Elsevier B.V. All rights reserved.
http://dx.doi.org/10.1016/j.gloplacha.2012.08.003

by a general pattern of reduced rainfall in equatorial West Africa (Nguetsop et al., 2004; Shanahan et al., 2009), but with timing and intensity varying regionally. In the Sahel region, paleoclimatic patterns remain unclear, especially during the DACP. Some records show wetter conditions (Bouimetarhan et al., 2009), whereas other records suggest that the climate was generally dry (Holmes et al., 1998; Stokes et al., 2004; Mulitza et al., 2010; Nizou et al., 2011). Additional paleoclimate records are needed in the Sahel to understand the centennial variability of the monsoon influence in this highly sensitive region.

Mollusk shells have been shown to be faithful environmental archives (Goodwin et al., 2001; Carré et al., 2005; Schöne et al., 2005; Lazareth et al., 2006; Yamamoto et al., 2010; Batenburg et al., 2011; Carré et al., 2012a; Sadler et al., 2012).

In this study, we present a multi-decadal reconstruction of the past hydrological variations from AD 460 to 1090 in the hypersaline Saloum Delta, Senegal, based on oxygen stable isotopes measured in modern and fossil *Anadara senilis* mollusk shells.

2. Regional settings

The Saloum Delta is located about 100 km south of Dakar (Senegal), between 13°40′N and 14°20′N, in the western part of the Sahel (Fig. 1). It is connected to the Atlantic Ocean by three main channels: the Saloum, the Diomboss and the Bandiala. The area between the channels consists of mangrove islands interconnected by a dense network of smaller channels (Simier et al., 2004). The estuary was an open bay 6000 years ago and was progressively filled with sediments to reach, between 2000 and 1500 BP a geomorphology similar to the modern one with large mangrove islands and beach barriers (Ausseil-Badie et al., 1991; Barusseau et al., 1995; Diara and Barusseau, 2006). A last infilling phase took place between 1500 BP and 600 BP. The formation of sand and mud flats allowed the ancient fishermen settlement and the edification of shell middens.

The Saloum catchment basin is very small compared to other West African rivers. Its total area (29,720 km^2) lies within Senegal and under the Soudano-Sahelian climate zone (Diouf, 1996). This means that hydrological changes in the Saloum estuary have a local origin. Mean precipitation ranged from 600 to 800 mm/yr during the 1950s, and dropped at about 500 mm/yr by the end of the 1960s (Dacosta, 1993; Mbow et al., 2008; Salack et al., 2011). In general, rainfall occurs only during the monsoon season, from July to September, when the ITCZ is at its northernmost position. This rainy season is followed by a long dry season for the rest of the year (Nicholson, 2000; Mbow et al., 2008). The highly negative annual precipitation–evaporation budget (P–E) combined with tidal sea-water incursions induced hypersaline conditions in the estuary (Diouf, 1996). The Saloum estuary is thus an inverse "tide influenced" estuary, with salinity increasing upstream (Pagès and Citeau, 1990; Simier et al., 2004; Mikhailov and Isupova, 2008). Measurements made during the dry season by Diop (1986) showed a gradual increase of salinities from 36 psu at the river mouth to 125 psu at Kaolack, 120 km from the coast. However, a transient normal salinity gradient (salinity decreasing upstream) is generally observed during and just after the rainy season in the mangrove Delta (Villanueva, 2004; Gning-Cisse, 2008; Azzoug et al., 2012). This drop of salinity is mainly due to direct rainfall and perhaps to groundwater since the river discharge remains insignificant.

The salinity gradient in western Africa inverse estuaries increased sharply during the Sahel droughts in the 1960s (Savenije and Pagès, 1992). The salinity in Kaolack, increased at the rate of about 1.3 per year between 1950 and 1986 (Pagès and Citeau, 1990). This shows that the water salinity in the Saloum (and thus the water $\delta^{18}O$ to which it is strongly correlated) is highly sensitive to multi-decadal variations of the monsoon.

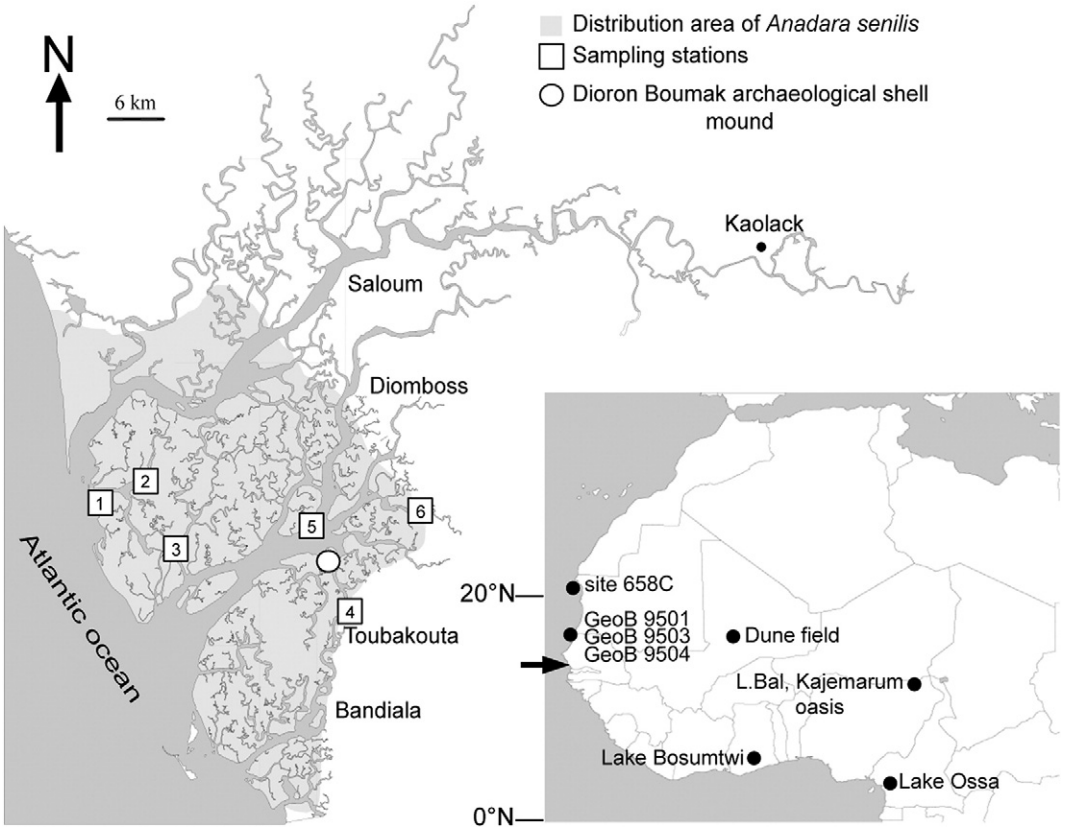

Fig. 1. Map of the Saloum Delta, indicating the *Anadara senilis* distribution area, the location of the sampling sites, and the shell midden Dioron Boumak studied here. Bottom right: map of Western Africa with the location of paleoclimate records mentioned in the text. Our study site is indicated by an arrow.

3. *A. senilis* (Linnaeus, 1758)

A. senilis is a common bivalve of the estuaries and coastal lagoons of the African Atlantic coast, from Rio de Oro (26°N) to Cap Frio (Angola, 18°S) (Nicklès, 1950). It forms dense banks in sandy to muddy sediments in the intertidal zone. This euryhaline species occurs as well in hypersaline zones like the Arguin Bank in Mauritania (S = 40) (Wolff et al., 1987) as well as in brackish conditions like the Benya lagoon in Ghana (S = 10) (Yankson, 1982; Otchere et al., 2003). In the Saloum Delta, *A. senilis* is the most common mollusk species (Elouard and Rosso, 1977) and is abundantly found in archeological shell middens (Thilmans and Descamps, 1982). Sclerochronological patterns have been studied in modern and fossil shells in this estuary by Azzoug et al. (2012). This study revealed that Dioron Boumak fossil shells grew year round without interruption despite a lower growth rate during the monsoon season. Growth patterns in modern shells were not distinct enough to estimate seasonal growth rate variations, but recent isotopic profiles (not shown) suggest that seasonal variability is also recorded, with a decreasing growth rate in the dry season. As a result, average $\delta^{18}O$ values in modern (fossil) shells are expected to be slightly underestimated (overestimated).

4. Material and methods

4.1. The Dioron Boumak shell midden chronology

The numerous archeological shell middens found in the mangrove islands of the Saloum Delta are evidence of ancient human occupation and intense shellfish gathering activity. This shellfish-based economy was observed and mentioned in the narratives of European explorers, compiled by Valentim Fernandes in the 16th century. They highlighted the economical importance of shellfish for local consumption and for trade. Shells were locally gathered, processed, smoked and their flesh were transported in potteries for long distance trading activity. This type of exploitation was likely representative of the preceding two millennia according to the archeological observations of Descamps and Thilmans (1979). These authors interpreted the large fast-accumulating Saloum shell middens as production sites dedicated to a shellfish trade with inland tribes.

The Dioron Boumak shell deposit is one of the largest anthropogenic shell middens in the Saloum Delta. Mollusk shell accumulation formed a 10 m high artificial island of approximately 10 ha (Descamps et al., 1974). After the site was abandoned, the eastern side of the shell mound was eroded by tides, forming a vertical cliff where the complete stratigraphy is exposed (Fig. 2). The deposit is composed primarily of mollusk shells, almost exclusively represented by *A. senilis*. Infilling sediment is composed of fine sand, silt, charcoal and ashes from fire pits used to process the bivalves.

Eight AMS radiocarbon dates were obtained from charcoal fragments collected from the vertical cliff of the Dioron Boumak shell midden (Table 1). The age model of the shell middens was constructed using the *Clam* code of Blaauw (2010). This code calibrates first the ^{14}C dates using the IntCal09 calibration data (Reimer et al., 2009), generates a best fit age model based on linear interpolation between the radiocarbon dates, and estimates the age error bar (Fig. 3). Based on this age model, the Dioron Boumak site was occupied from ~AD 460 to 1360 (Fig. 3). However, our sampling only covers the period between AD 460 and 1090, corresponding roughly to the DACP and part of the MWP. Two phases of edification can be distinguished: a first phase of fast edification rate (~200 cm/century) from 10 to 2 m depth, followed by a slower accumulation phase (~40 cm/century) for the two upper meters (Fig. 3).

Anthropogenic shell middens generally have complex depositional histories. However, several indications support that the Dioron Boumak edification was continuous. First, the 8 dates of the age model are in stratigraphic order. Secondly, we did not observe any soil layer or eolian deposit in the middens section that could indicate a site abandonment of a few decades. Third, the continuity of shell accumulation is supported by the hypothesis that this site was devoted to industrial production (Descamps and Thilmans, 1979) which implies a regular long-term activity. This was confirmed by our own observations in the Dioron Boumak section: (1) we found no sign of stratigraphic perturbation, (2) the density of cultural remains was low, and (3) shells were not fragmented suggesting a low trampling rate. Finally, it is unlikely that shell gathering was restricted to anomalously wet or dry conditions because this species lives in a very wide range of hydrological conditions

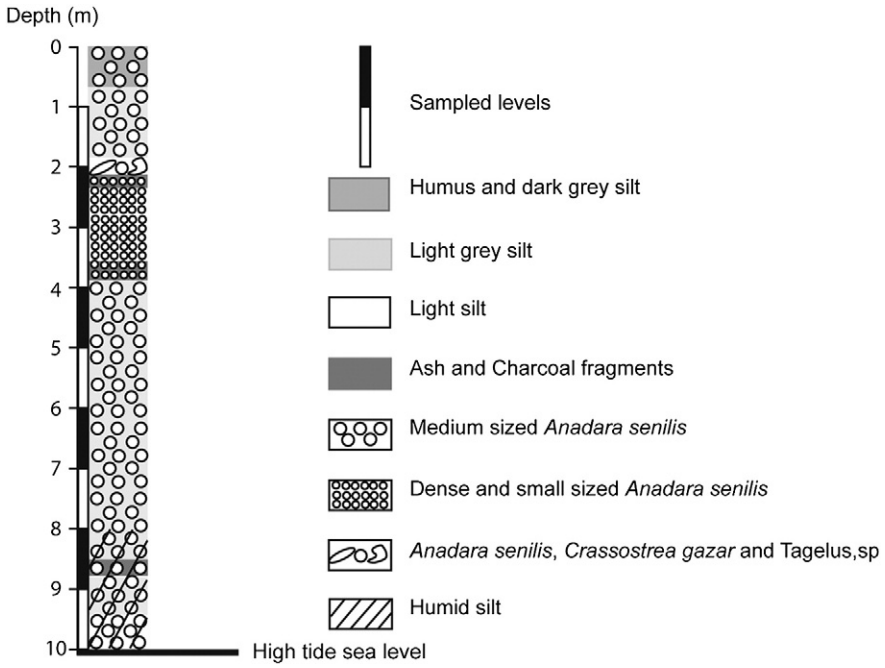

Fig. 2. Stratigraphic profile of the Dioron Boumak shell midden.

Table 1
Summary of radiocarbon dates on charcoal from the Dioron Boumak shell midden.

Lab. N°	Depth (m)	^{14}C ages (yrs BP)	1-σ calibrated range (yrs AD)	2-σ calibrated range (yrs AD)	Median calibrated ages (yrs AD)
UBA 19943	0.5	817±23	1215–1256	1179–1265	1229
UBA 19944	1.5	1083±38	897–1011	890–1019	957
SacA 25596	2.4	1195±35	779–881	694–947	829
SacA 25597	3.6	1260±30	689–775	669–862	736
SacA 25598	4.8	1270±30	688–771	664–856	729
SacA 25599	6.7	1370±30	644–669	608–688	655
SacA 25600	8.5	1480±30	557–613	541–642	587
SacA 25601	9.25	1530±30	441–578	432–600	537

and has been gathered in the past from Mauritania (Barusseau et al., 2007) to Gabon (Van Neer and Clist, 1991). Thus, shell deposition was likely rather continuous all along the studied period. It has probably been interrupted occasionally for some months or years, but this is not expected to affect significantly the paleoenvironmental record on multidecadal timescales.

4.2. Shell material

Fossil shells were sampled on the Dioron Boumak shell midden, along the same outcrop that was dated. After cleaning the outcrop, shell samples were collected in nine successive 1 m high sections from 1 m below the surface down to the base (10 m), which corresponds to the sea level (Fig. 2). The upper meter was not sampled because of the high shell fragmentation rate. Six shells from every section were analyzed. The successive sampled sections yield a temporal resolution ranging between 14 and 97 years, with an average of ~50 years for the first accumulation phase (2 to 10 m depth) and a lower temporal resolution of about 205 years for the last sampled level (1 to 2 m depth). For modern analogs, 30 live specimens of *A. senilis* were collected in May 2010 and May 2011 during low tide on intertidal mudflats in six sites from the estuary mouth to the limit of the species distribution (Fig. 1, sites 1 to 6).

4.2.1. Diagenesis tests

In order to investigate the preservation state of fossil shells, X-ray diffraction analyses were performed on hinge fragments of modern and fossil shells of every sample. A PanAnalytical X'Pert diffractometer (Cu-Kα, 40 kV, 20 mA, 2θ range from 20 to 55° with step size of 0.02°) was used. The XRD spectra showed that modern and fossil shells' calcium carbonate was pure aragonite, which suggests that shell hinges were not affected by recrystallization. In addition, the shell microstructure of the hinge and the outer layer was examined in a modern and a fossil shell using a Cambridge Stereoscan-360® at 15 kV scanning electron microscope (SEM). The fossil shell exhibited a very well-preserved crossed-lamellar micro-structure similar to the modern shells. These diagenesis tests showed that the aragonite in fossil shells was well preserved, and thus suitable for isotopic analyses.

4.2.2. Shell preparation and isotopic analyses

Shells were embedded in polyester resin and sectioned radially along the axis of maximum growth using a low speed saw with diamond

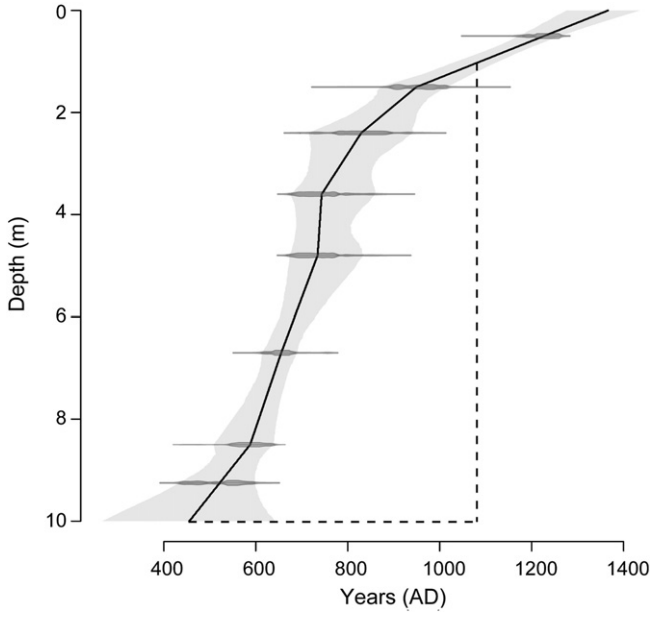

Fig. 3. Dioron Boumak shell midden age model produced by the *Clam* software (Blaauw, 2010). The grey envelope shows the 2σ age envelope. Dashed lines indicate the levels and the period covered by our sampling.

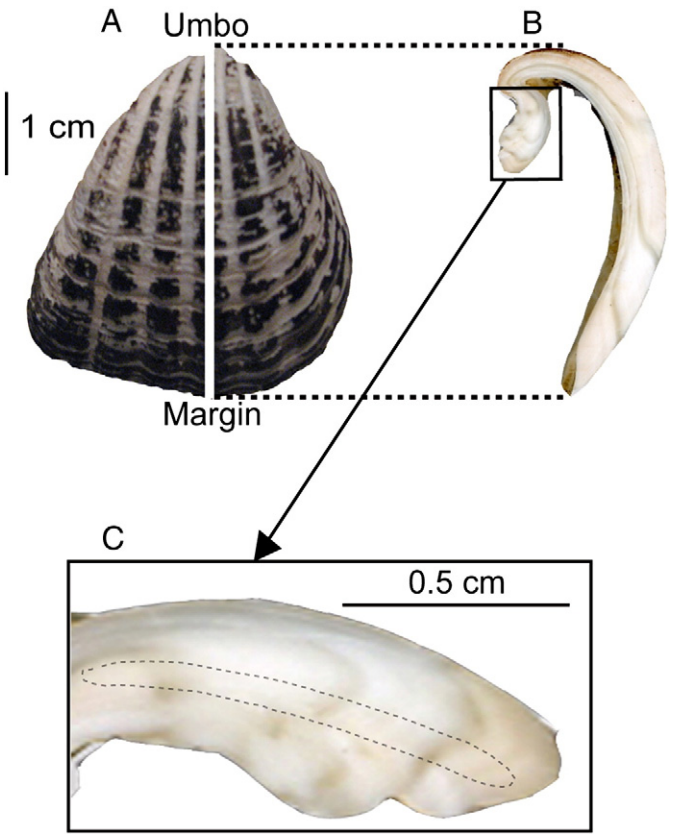

Fig. 4. (A) *Anadara senilis* valves were cut along the axis of maximum growth. (B) *A. senilis* polished radial section. This fossil shell lived about 3 years as indicated by the three dark bands formed during monsoon seasons. (C) Microsamples (typically a 0.2 mm deep groove as shown by the dotted line) were taken across the hinge plat to include most of the shell lifespan. The monsoon-related growth bands can also be observed in the hinge plat.

wafering blade. Millimetre-thick sections were mounted on glass slides and polished with 1 μm Al_2O_3 (Fig. 4B).

For each shell, a microsample of aragonite powder (~0.2 mg) integrating most of the specimen lifetime was extracted for isotopic analysis from the hinge using an automated microdrill (Fig. 4C). The stable isotopic composition of the carbonate powder samples was analyzed at the University of Washington Isolab using a dual inlet Finnigan DeltaPlus isotope ratio mass spectrometer coupled to a Kiel III carbonate device (standard deviation for repeated measurements of the internal standard was better than 0.08‰ for $\delta^{18}O$). Part of the samples was analyzed in the LOCEAN laboratory, Paris, using a Dual Inlet Isoprime mass spectrometer (standard deviation for repeated measurements of the internal standard was better than 0.05‰ for $\delta^{18}O$. $\delta^{18}O$ was reported with respect to Vienna Pee Dee Belemnite (VPDB) scale using NBS19 ($\delta^{18}O = -2.2‰$) and NBS18 ($\delta^{18}O = -23.01‰$) (Coplen, 1994; Coplen et al., 2006) to measure internal laboratory standards run alongside samples. Oxygen isotope data were corrected according to Kim et al. (2007) using an aragonite-phosphoric acid fractionation factor ($\alpha = 1.0090901$ at 70 °C) and calcite-phosphoric acid fractionation factor ($\alpha = 1.0087096$ at 70 °C) to account for the aragonitic nature of the samples. Eq. (1) yields a correction of −0.38‰ at 70 °C for aragonite samples.

$$\delta^{18}O_{Aragonite} = \frac{\alpha_{CO_2(ACID)-Calcite}}{\alpha_{CO_2(ACID)-Aragonite}} \cdot \left(\delta^{18}O_{Calcite} + 1000\right) - 1000. \quad (1)$$

4.3. Water sampling and analysis

Temperature and salinity of the water were measured *in situ* in the six sites where the modern shells were gathered and water samples were taken to analyze their oxygen isotopic composition ($\delta^{18}O_W$). Water samples were also collected weekly at high tide at Toubakouta (site 4 in Fig. 1) from November 2010 to November 2011.

The oxygen isotopic composition of the water samples was measured in the HydroScience Montpellier laboratory using a dual inlet Isoprime isotope ratio mass spectrometer using the classical CO_2-H_2O equilibration method (Cohn and Urey, 1938). Saline waters and accompanying standards were equilibrated with CO_2 for 24 h at 35 °C. The standard deviation for repeated measurements of an internal standard was 0.15‰. Water oxygen isotope ratios are reported with respect to Vienna Standard Mean Ocean Water (VSMOW). VSMOW ($\delta^{18}O = 0‰$) and SLAP ($\delta^{18}O = -55.5‰$) international standards were used to calibrate internal laboratory standards.

5. Results

5.1. Seasonality of water $\delta^{18}O$ in the Saloum Delta

The seasonal variations of water $\delta^{18}O$ ($\delta^{18}O_W$) in the Saloum from November 2010 to November 2011 are shown in Fig. 5. The dataset shows an annual range of 2.4 to 2.6‰, with more positive monthly values from April to June (1.6 to 2.03‰) and more negative values from September to November (0.07 to −0.57‰). This seasonal shift in $\delta^{18}O_W$ indicates seasonal variations in precipitation–evaporation budget, with inputs of isotopically light fresh water during the monsoon season and enrichment due to local evaporation during the dry season.

5.2. Spatial gradients of salinity and water $\delta^{18}O$

Salinity and $\delta^{18}O_W$ values of May 2010 and May 2011 in the modern sampling sites are represented in Fig. 6. Salinity ranged between 36.0 in site 1 and 49.5 in site 6 at the distribution limit of *A. senilis* (Fig. 6A). $\delta^{18}O_W$ values increased from 0.87‰ in site 1 to 3.21‰ in site 6 (Fig. 6B). As expected, there is a strong linear correlation between salinity and $\delta^{18}O_W$ ($R^2 = 0.8$, p-value = 0.01, $\alpha = 0.05$). The $\delta^{18}O_W$ in site 1 was slightly enriched in ^{18}O compared to the ocean water (~0.8‰,

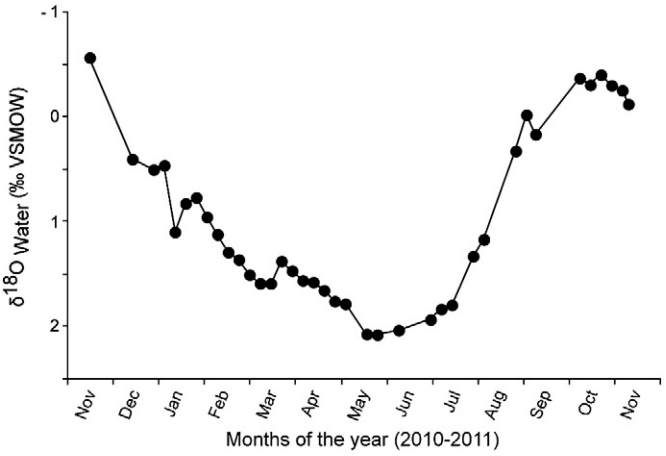

Fig. 5. Weekly $\delta^{18}O$ values of estuarine water at Toubakouta.

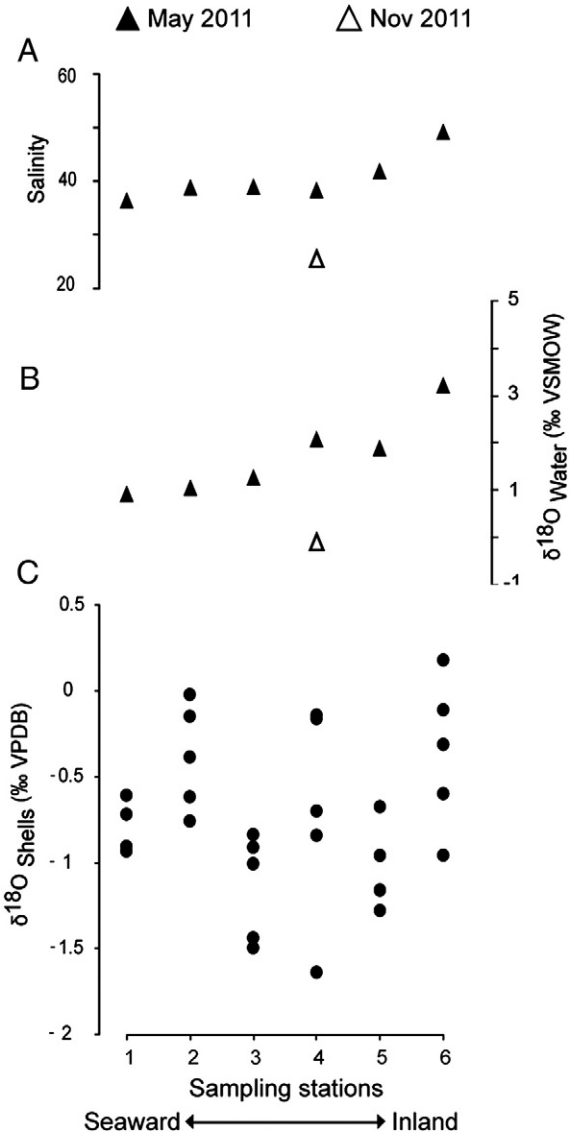

Fig. 6. Results obtained along a longitudinal transect (Fig. 1) for: (A) salinity in the dry season (May 2011) (black triangles) and after the rainy season (November 2011) (open triangle), (B) $\delta^{18}O_W$ in May 2011 (black triangles) and November 2011 (open triangles), (C) shell $\delta^{18}O$ mean values. Sampling sites are indicated on the X-axis (Fig. 1).

Legrande and Schmidt, 2006) and this enrichment increased inland as a result of increasing evaporation effect. However, these gradients only represent the month of May which corresponds to the end of the dry season when the evaporation effect is the highest. Analyses of water sampled in site 4 just after the rainy season in 2011 showed lower values of salinity and $\delta^{18}O_W$, below the ocean conditions (Fig. 6A, B). Other studies have shown briefly normal salinity gradient (decrease trend in salinity landward) during and just after the monsoon season (Villanueva, 2004; Gning-Cisse, 2008). In this area, the salinity and water $\delta^{18}O$ gradients, which are governed by the balance between freshwater inputs and evaporated seawater, are weaker during the rainy season and strengthen slightly during the dry season.

5.3. Modern shells' $\delta^{18}O$ values

The shell values range from −1.64‰ to 0.18‰, with mean values for sampling sites ranging from −1.14‰ to −0.36‰ (Fig. 6C). We observe no significant difference between shell values from site 1 to site 6 (Fig. 6C). While salinity and water $\delta^{18}O$ showed a positive gradient landward in May 2011, no significant gradient was observed in modern shells' $\delta^{18}O$ values because shells integrate hydrological conditions over 1 to 3 years, including periods of positive gradient during dry seasons and periods of negative gradient during the rainy season. An important scattering of isotopic values is observed within sampling sites, with total ranges of 0.33‰ in site 1 to 1.5‰ in site 4.

5.4. Fossil shells $\delta^{18}O$ values

Fossil shells $\delta^{18}O$ displayed values ranging between −3.29‰ and −1.04‰ (Fig. 7). Mean values from the successive levels ranged from −2.42‰ to −1.89‰. The mean values between the fossil levels are not significantly different (Kruskal Wallis test, p-value = 0.369).

The overall average $\delta^{18}O$ value of the fossil record was −2.11‰ (σ = 0.45‰, n = 54) and was depleted by ~1.4‰ compared with the modern average value of −0.74 (σ = 0.45‰, n = 30) (Fig. 7). This difference between fossil and modern shells is statistically significant (t-test, p-value = $2.2 * 10^{-16}$).

6. Discussion

The $\delta^{18}O$ in mollusk shells is governed by the temperature and the $\delta^{18}O$ of water in which bivalves precipitate their shell (Urey, 1947; Epstein et al., 1953; Grossman and Ku, 1986; Carré et al., 2005). To check whether *A. senilis* precipitates its aragonitic shell in equilibrium with ambient water, we compared the mean $\delta^{18}O$ measured on shells collected live in Toubakouta (−0.70‰ ± 0.61, n = 5) with a simulated shell $\delta^{18}O$ value calculated for Toubakouta using Grossman and Ku's (1986) Eq. (2) with a mean annual water temperature of ~26 °C (Simier et al., 2004) and a mean annual $\delta^{18}O_W$ of 0.97‰ (n = 38).

$$T(^{\circ}C) = 19.7 - 4.34 \cdot \left(\delta^{18}O_{\alpha\_aragonite} + 0.34 - \delta^{18}O_w\right) \quad (2)$$

where $\delta^{18}O_{\alpha\_arag}$ and $\delta^{18}O_{water}$ are expressed *vs* V-PDB and V-SMOW respectively. This equation was modified considering a constant correction of −0.34‰ calculated with Eq. (1) and acid-CO_2 fractionation factors calculated for a 50 °C temperature reaction (Kim et al., 2007).

The calculated value was −0.82‰, which lies within the error bar of the measured value and indicates that *A. senilis* precipitates its shell close to isotopic equilibrium with ambient water as was shown previously (Debenay and Fontes, 1994; Lavaud, 2010).

Modern shells were collected together and experienced the same environmental conditions. The scattering of isotopic values within sites (σ = 0.30‰) provides an estimate of the uncertainty related to this method for reconstructing annual mean conditions. This uncertainty can be mainly attributed to variations of the relative contribution of rainy seasons (characterized by negative shell $\delta^{18}O$ values) and dry seasons (characterized by positive shell $\delta^{18}O$ values) in the shell hinge carbonate samples. These variations can be due to different number of seasons included in the average value and to varying growth rates. Micro-scale environmental variability within sampling sites could additionally contribute to the observed scattering.

Mean fossil shells isotopic composition was depleted by 1.4‰ compared to the average value of modern shells. This difference could not be due to changes in shell growth seasonality since this effect would on the contrary tend to underestimate this shift (see Section 3).

If $\delta^{18}O_W$ was constant through time, this isotopic difference would correspond to a warming of more than 6 °C, which is unrealistic at this time scale, and inconsistent with SST reconstructions off the western African coast (core 658C and core GeoB 9501), showing that both the DACP and the MWP conditions were not significantly different from modern conditions (deMenocal et al., 2000; Kuhnert and Mulitza, 2011). A 1.4‰ variation of the ocean water isotopic composition is also unrealistic at this timescale considering that it is larger than the amplitude of variation for glacial–interglacial changes (Duplessy et al., 2002). Consequently, the depleted isotopic values in the Dioron Boumak fossil shells have to be primarily attributed to isotopically light mean values of $\delta^{18}O_W$ in the Saloum Delta.

The average $\delta^{18}O$ of the whole fossil record (−2.11‰) was more negative than the most negative of the modern shells (−1.64‰) in the Saloum Delta. Considering a mean temperature value of 26 °C in Eq. (2), the average fossil isotopic value corresponds to a $\delta^{18}O_W$ value of ~−0.32‰. This water isotopic value is significantly more negative

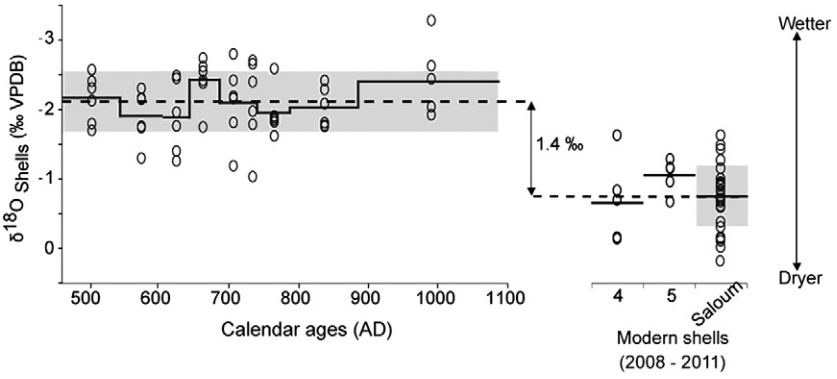

Fig. 7. $\delta^{18}O$ values of *Anadara senilis* shells from the archeological site Dioron Boumak compared to modern shells. Values of individual shells are indicated by open circles. For each sample, the mean value was indicated by a solid black line. The time interval represented by successive samples was estimated from the age model. For the modern shells, values from sites 4 and 5 (closest to the shell middens) and for the whole estuary are represented separately. In addition, the mean values of the whole fossil dataset and the modern dataset are represented by dashed lines, with the associated standard deviation (grey area). Negative values indicate increased influence of freshwater (reversed scale).

than the modern $\delta^{18}O_W$ value measured in the Saloum (0.97‰) and also than the mean $\delta^{18}O_W$ in the bordering ocean (~0.8‰) (Legrande and Schmidt, 2006). This is a strong indication that the water in the Saloum Delta was brackish most of the year rather than hypersaline during the studied period. It means that the inverse salinity gradient observed today in the Saloum Delta appeared after AD 1090.

$\delta^{18}O_W$ in the Saloum Delta is controlled by freshwater inputs from monsoon precipitation and groundwater, marine water tidal incursions and evaporation (Diop, 1986; Dacosta, 1993; Faye et al., 2005). A decreased annual evaporation rate may have contributed to the lower values of $\delta^{18}O_W$. Available data of evaporation rate in the Saloum region show that the minimum and maximum monthly evaporation rates occur in September (67 mm) and March (312 mm) respectively, and are strongly related to the monsoon cloud cover (Dacosta, 1993). Since temperature and solar activity did not change significantly during the studied period, a hypothetical reduction in annual evaporation would have been primarily the result of a longer monsoon season.

Weaker marine incursions could have contributed to the observed lower values of estuarine water $\delta^{18}O_W$. Since the Delta geomorphology was already similar to the actual one (see Section 2), changes in marine incursions would have been primarily due to sea level changes. Faure et al.'s (1980) sea level reconstructions in Senegal discussed later by Nizou et al. (2010) suggest a slightly higher sea level (0–50 cm) during the studied period. The isotopic impact of stronger marine incursions would be a dampening of the $\delta^{18}O_W$ seasonal variations, with a mean value closer to the ocean isotopic value (~0.8‰). This means that, under these conditions, annual freshwater input into the Saloum Delta was significantly larger than today to compensate for the marine influence and reach a mean $\delta^{18}O_W$ value of −0.32‰.

Thus, our results strongly suggest that the annual freshwater input into the Saloum Delta was substantially larger between AD 460 and 1090 than it is today, which means that the monsoon was stronger and/or longer than today in the Saloum catchment basin. The isotopic effect of the rainfall might have been increased by lower evaporation due to an increased duration of the monsoon.

The successive sections sampled in the shell middens represent time slices of approximately 50 years in the first phase and 205 years for the uppermost section. The mean hydrological conditions in every section were estimated by the average isotopic value obtained from a random sample of 6 shells. Statistically, a sample of 6 shells spanning1 to 3 years is large enough to provide a representative estimate of mean climate conditions but is too small to capture interannual variability (Carré et al., 2012b). Some short-term inter-annual to decadal droughts could have occurred without being apparent in our proxy record, either because they were averaged with wetter periods, or because they could be missing from our random shell samples. However, a multi-decadal drought similar to the one that has been recently observed in the Sahel would have influenced the hydrological conditions over a period that would exceed the record resolution. Such climatic events would have been likely detected in the shell isotopic record. The insignificant variability between successive samples suggests that the multi-decadal to centennial monsoon variability was low at least for the 8 first levels from AD 460 to 883 (Fig. 7). It seems unlikely that any large scale climatic event similar to the recent Sahel drought (with annual precipitation of 500 to 600 mm in the Saloum basin over ~4 decades) occurred during these ~430 years.

We do record a prominent regional increase in the precipitation–evaporation budget between the time the site was occupied (AD 460 to 1090) and now. The closest high resolution paleoenvironmental records were obtained from sediment cores off the Senegal River mouth, namely GeoB 9501, 9503 and 9504. During the DACP, fresher conditions in the Senegal River estuary were inferred from a higher concentration of freshwater algae (Bouimetarhan et al., 2009) while drier conditions were inferred at the catchment basin scale from geochemical analyses (Nizou et al., 2011). Aeolian dust deposition in the sediments also indicated dry conditions at larger geographic scale (Mulitza et al., 2010). Further east in a similar latitudinal range, aridity was suggested in Mali by eolian dune reactivation (Stokes et al., 2004), and in northern Nigeria by saline conditions in the Kajemarum oasis (Holmes et al., 1998). It seems thus that humid conditions may have been restricted in the Sahel to the Atlantic coastal zone, while drier conditions prevailed in the rest of the Sahel and in Equatorial West Africa. This period seems thus characterized by a significant change in evaporation and/or rainfall distribution that could not be attributed to a latitudinal displacement of the ITCZ.

The spatial pattern is modified during the MWP, when most proxy records from the Sahel show increased humidity from the Senegal coast to Northern Nigeria (Holmes et al., 1999; Stokes et al., 2004; Mulitza et al., 2010; Nizou et al., 2011). At the same time, equatorial West Africa was marked by a general pattern of drying as shown by low level of Lake Bosumtwi in Ghana (Shanahan et al., 2009) and of Lake Ossa in Cameroon (Nguetsop et al., 2004). This hydrological dipole between Equatorial West Africa and the Sahel during the MWP may be the result of a northward shift of the ITCZ as it has been suggested in many localities in the tropics (Verschuren et al., 2000; Haug et al., 2001; Poore et al., 2004; Stager et al., 2005). Today, the Atlantic Multidecadal Oscillation (AMO) is closely linked to Sahel precipitation and to the position of the ITCZ at multidecadal time scales (Folland et al., 1986; Knight et al., 2006; Zhang and Delworth, 2006). Proxy records from the North Atlantic show a long lasting positive phase of AMO during the MWP (Feng et al., 2009, 2010; Mann et al., 2009; Knudsen et al., 2011), which supports the hypothesis that the rainfall anomaly observed in West Africa during the MWP may be forced by North Atlantic SSTs.

7. Conclusion

We used the isotopic composition of fossil shells of *A. senilis* from the massive shell midden Dioron Boumak as a proxy to reconstruct hydrological conditions in the Saloum estuary area in Senegal. $\delta^{18}O$ values from fossil shells covering the period AD 460-1090 were depleted by ~1.4‰ compared to modern shells. This result indicates that the Saloum estuary was likely not hypersaline as it is today but brackish because of a substantially more positive annual precipitation-evaporation budget during this period due to increased monsoon precipitation and/or reduced annual evaporation. It seems that monsoonal precipitation was relatively stable at the multi-decadal to centennial time scale during this period. No prominent multidecadal drought similar to the 20th century event was detected in the Dioron Boumak record for this ~600 year interval. Comparisons with paleoclimate records from West Africa suggest that wetter conditions were restricted to the coastal Senegal during the DACP and then extended through the Sahel during the MWP, possibly in response to a long-lasting positive AMO-like phase.

Acknowledgments

We would like to thank Jean Raffray, François Sanseo, Ansou Mané, Cesar Tendeng and Bernard Bassène of the IRD of Dakar for their assistance during field work. We are thankful to Cyr Descamps for sharing his knowledge about archeological shell middens in the Saloum. We thank N. Patris and HydroSciences of Montpellier for $\delta^{18}O$ analyses.

We are also grateful to two anonymous reviewers for their valuable comments. This work was supported by the INSU-LEFE/EVE program (SALOUM project, P.I. M. Carré). This is ISEM contribution no. 2012-084.

References

Ausseil-Badie, J., Barusseau, J.P., Descamps, C., Diop, E.H.S., Giresse, P., Pazdur, M., 1991. Holocene deltaic sequence in the Saloum Estuary, Senegal. Quaternary Research 36, 178–194.

Azzoug, M., Carré, M., Schauer, A.J., 2012. Reconstructing the duration of the West African Monsoon season from growth patterns and isotopic signals of shells of *Anadara senilis* (Saloum Delta, Senegal). Palaeogeography, Palaeoclimatology, Palaeoecology 346–347, 145–152.

Barusseau, J.P., Bâ, M., Descamps, C., Diop, E.H.S., Giresse, P., Saos, J.L., 1995. Coastal evolution in Senegal and Mauritania at 10^3, 10^2 and 10^1-year scales: natural and human records. Quaternary International 29/30, 61–73.

Barusseau, J.P., Vernet, R., Saliège, J.F., Descamps, C., 2007. Late Holocene sedimentary forcing and human settlements in the Jerf el Oustani-Ras el sass region (Banc d'Arguin, Mauritania). Geomorphologie: Relief, Processus, Environnement 7, 7–18.

Batenburg, S.J., Reichart, G.J., Jilbert, T., Janse, M., Wesselingh, F.P., Renema, W., 2011. Interannual climate variability in the Miocene: high resolution trace element and stable isotope ratios in giant clams. Palaeogeography, Palaeoclimatology, Palaeoecology 306, 75–81.

Blaauw, M., 2010. Methods and code for classical age-modelling of radiocarbon sequences. Quaternary Geochronology 5, 512–518.

Bouimetarhan, I., Dupont, L., Schefuß, E., Mollenhauer, G., Mulitza, S., Zonneveld, K., 2009. Palynological evidence for climatic and oceanic variability off NW Africa during the late Holocene. Quaternary Research 72, 188–197.

Carré, M., Bentaleb, I., Blamart, D., Ogle, N., Cardenas, F., Zevallos, S., Kalin, R., Ortlieb, L., Fontugne, M., 2005. Stable isotopes and sclerochronology of the bivalve Mesodesma donacium: potential application to Peruvian paleoceanographic reconstructions. Palaeogeography, Palaeoclimatology, Palaeoecology 228, 4–25.

Carré, M., Azzoug, M., Bentaleb, I., Chase, B.M., Fontugne, M., Jackson, D., Ledru, M.-P., Maldonado, A., Sachs, J.P., Schauer, A.J., 2012a. Mid-Holocene mean climate in the south eastern Pacific and its influence on South America. Quaternary International 253, 55–66.

Carré, M., Sachs, J.P., Wallace, J.M., Favier, C., 2012b. Exploring errors in paleoclimate proxy reconstructions using Monte Carlo simulations: paleotemperature from mollusk and coral geochemistry. Climate of the Past 8, 433–450.

Charney, B.J.G., 1975. Dynamics of deserts and drought in the Sahel. Quarterly Journal of the Royal Meteorological Society 101, 193–202.

Cohn, M., Urey, H.C., 1938. Oxygen exchange reactions of organic compounds with water. Journal of the American Chemical Society 60, 679–687.

Coplen, T.B., 1994. Reporting of stable hydrogen, carbon, and oxygen isotopic abundances. Pure and Applied Chemistry 66, 273–276.

Coplen, T.B., Brand, W.A., Gehre, M., Gröning, M., Meijer, H.A.J., Toman, B., Verkouteren, R.M., 2006. New guidelines for $\delta^{13}C$ measurements. Analytical Chemistry 78, 2439–2441.

Dacosta, H., 1993. Variabilité des précipitations sur le bassin versant du Saloum. Gestion des ressources côtières et littorales du Sénégal. Actes de l'atelier de Gorée 27-29 juillet 1992, pp. 87–103.

Dai, A., Trenberth, K.E., Qian, T., 2004a. A global dataset of Palmer Drought Severity Index for 1870–2002: relationship with soil moisture and effects of surface warming. Journal of Hydrometeorology 5, 1117–1130.

Dai, A., Lamb, P.J., Trenberth, K.E., Hulme, M., Jones, P.D., Xie, P., 2004b. The recent Sahel drought is real. International Journal of Climatology 24, 1323–1331.

Davidson, O., Halsnæs, K., Huq, S., Kok, M., Metz, B., Sokona, Y., Verhagen, J., 2003. The development and climate nexus: the case of sub-Saharan Africa. Climate Policy 3, 97–113.

Debenay, J.P., Fontes, J.C., 1994. Isotopic evolution of fluids and biogenic aragonite in an intertropical coastal lagoon — possible use for paleoenvironmental studies. Comptes Rendus de l'Académie des Sciences 318, 1087–1094.

deMenocal, P., Ortiz, J., Guilderson, T., Sarnthein, M., 2000. Coherent high- and low-latitude climate variability during the Holocene warm period. Science 288, 2198–2202.

Descamps, C., Thilmans, G., 1979. les tumulus coquillers des iles du Saloum (Senegal). Bulletin de Liaison de l'Association Sénégalaise pour l'Etude du Quaternaire de l'Ouest africain 54–55, 81–91.

Descamps, C., Thilmans, G., Thommeret, Y., 1974. Données sur l'édification de l'amas coquillier de Dioron Boumak (Senegal). Bulletin de Liaison de l'Association Sénégalaise pour l'Etude du Quaternaire de l'Ouest africain 41, 67–83.

Diara, M., Barusseau, J.P., 2006. Late Holocene evolution of the Saloum–Gambia double delta (Senegal). Geo-Eco-Marina 12, 17–28.

Diop, E.S., 1986. Tropical holocene estuaries. Comparative study of the physical geography features of the rivers from the south of Saloum to the Mellcorée (Guinea Republic). Ph.D. Thesis, Université Louis Pasteur, Strasbourg, France.

Diouf, P.S., 1996. Les peuplements de poissons des milieux estuariens de l'Afrique de l'ouest: l'exemple de l'estuaire hypersalin du Sine Saloum. Ph.D. Thesis, Université Montpellier II, Montpellier, France.

Duplessy, J.C., Labeyrie, L., Waelbroeck, C., 2002. Constraints on the ocean oxygen isotopic enrichment between the Last Glacial Maximum and the Holocene: paleoceanographic implications. Quaternary Science Reviews 21, 315–330.

Elouard, P., Rosso, J.C., 1977. Biogéographie et habitat des mollusques actuels lagunomarins du delta du Saloum (Sénégal). Geobios 10, 275–296.

Epstein, S., Buchsbaum, R., Lowenstam, H.A., Urey, H.C., 1953. Revised carbonate water isotopic temperature scale. Bulletin of the Geological Society of America 64, 1315–1326.

Faure, H., Fontes, J.C., Hebrard, L., Monteillet, J., Pirazzoli, P.A., 1980. Geoidal change and shore-level tilt along Holocene estuaries: Sénégal River Area, West Africa. Science 210, 421–423.

Faye, S., Maloszewski, P., Stichler, W., Trimborn, T., Cissé-Faye, S., Bécaye-Gaye, C., 2005. Groundwater salinization in the Saloum (Senegal) delta aquifer: minor elements and isotopic indicators. The Science of the Total Environment 343, 243–259.

Feng, S., Hu, Q., Oglesby, R.J., 2009. AMO-like variations of Holocene sea surface temperature in the North Atlantic Ocean. Climate of the Past Discussion 5, 2465–2496.

Feng, S., Hu, Q., Oglesby, R.J., 2010. Influence of Atlantic sea surface temperature on persistent drought in the North America. Climate Dynamics http://dx.doi.org/10.1007/s00382-010-0835-x.

Folland, C.K., Palmer, T.N., Parker, D.E., 1986. Sahel rainfall and worldwide sea temperatures, 1901–1985. Nature 320, 602–607.

Giannini, A., Saravanan, R., Chang, P., 2003. Oceanic forcing of Sahel rainfall on interannual to interdecadal time scales. Science 302, 1027–1030.

Gning-Cisse, N., 2008. Ecologie trophique des juveniles de quatres espèces de poissons dans l'estuaire inverse du Sine-Saloum(senegal): influence des conditions de salinité contrastées. Ph.D. Thesis, Université Montpellier II, Montpellier, France.

Goodwin, D.H., Flessa, K.W., Schone, B.R., Dettman, D.L., 2001. Cross-calibration of daily growth increments, stable isotope variation, and temperature in the Gulf of California bivalve mollusk *Chione cortezi*: implications for paleoenvironmental analysis. Palaios 16, 387–398.

Grossman, E.L., Ku, T.L., 1986. Oxygen and carbon isotope fractionation in biogenic aragonite: temperature effects. Chemical Geology (Isotope Geoscience Section) 59, 59–74.

Haug, G.H., Hughen, K.A., Sigman, D.M., Peterson, L.C., Röhl, U., 2001. Southward migration of the intertropical convergence zone through the Holocene. Science 293, 1304–1308.

Holmes, J.A., Fothergill, P.A., Street-perrott, F.A., Perrott, R.A., 1998. A high-resolution Holocene ostracod record from the Sahel zone of Northeastern Nigeria. Journal of Paleolimnology 20, 369–380.

Holmes, J.A., Allen, M.J., Street-perrott, F.A., Ivanovich, M., Perrott, R.A., Waller, M.P., 1999. Late Holocene palaeolimnology of Bal Lake, Northern Nigeria, a multidisciplinary study. Palaeogeography, Palaeoclimatology, Palaeoecology 148, 169–185.

Hulme, M., 2001. Climatic perspectives on Sahelian desiccation: 1973–1998. Global Environmental Change 11, 19–29.

IPCC, 2007. Climate Change 2007: the Physical Science Basis. Contribution of Working Group I to the Fourth Assessment Report of the Intergovernmental Panel on Climate Change (IPCC). Cambridge University Press, Cambridge.

Janicot, S., Trzaska, S., Poccard, I., 2001. Summer Sahel-ENSO teleconnection and decadal time scale SST variations. Climate Dynamics 18, 303–322.

Kim, S.T., Mucci, A., Taylor, B.E., 2007. Phosphoric acid fractionation factors for calcite and aragonite between 25 and 75 °C: revisited. Chemical Geology 246, 135–146.

Knight, J.R., Folland, C.K., Scaife, A.A., 2006. Climate impacts of the Atlantic multidecadal oscillation. Geophysical Research Letters 33, L17706 http://dx.doi.org/10.1029/2006GL026242.

Knudsen, M.F., Seidenkrantz, M.S., Jacobsen, B.H., Kuijpers, A., 2011. Tracking the Atlantic multidecadal oscillation through the last 8000 years. Nature Communications http://dx.doi.org/10.1038/ncomms1186.

Kuhnert, H., Mulitza, S., 2011. Multidecadal variability and late medieval cooling of near-coastal sea surface temperatures in the eastern tropical North Atlantic. Paleoceanography 26 http://dx.doi.org/10.1029/2011PA002130.

Lavaud, R., 2010. Exploration du potentiel de la coquille de l'arche Ouest-Africaine, *Anadara senilis*, comme archive paléo-environnementale. Master thesis. Université de Bretagne occidentale, Brest, France.

Lazareth, C.E., Lasne, G., Ortlieb, L., 2006. Growth anomalies in *Protothaca thaca* (Molluska, Veneridae) shells as markers of ENSO conditions. Climate Research 30, 263–269.

Lebel, T., Diedhiou, A., Laurent, H., 2003. Seasonal cycle and interannual variability of the Sahelian rainfall at hydrological scales. Journal of Geophysical Research 108, 1–11.

LeGrande, A.N., Schmidt, G.A., 2006. Global gridded data set of the oxygen isotopic composition in seawater. Geophysical Research Letters 33, L12604 http://dx.doi.org/10.1029/2006GL026011.

Ljungqvist, F.C., 2010. A new reconstruction of temperature variability in the extra-tropical northern hemisphere during the last two millenia. Geografiska Annaler 92A, 339–351.

Mann, M.E., Zhang, Z., Rutherford, S., Bradley, R.S., Hughes, M.K., Shindell, D., Ammann, C., Faluvegi, G., Ni, F., 2009. Global signatures and dynamical origins of the Little Ice Age and Medieval climate anomaly. Science 326, 1256–1260.

Mbow, C., Mertz, O., Diouf, A., Rasmussen, K., Reenberg, A., 2008. The history of environmental change and adaptation in eastern Saloum–Senegal – driving forces and perceptions. Global and Planetary Change 64, 210–221.

Mcdermott, F., Mattey, D.P., Hawkesworth, C., 2005. Centennial-scale Holocene Climate variability revealed by a high-resolution Speleothem $\delta^{18}O$ record from SW Ireland. Science 294, 1328–1332.

Mikhailov, V.N., Isupova, M.V., 2008. Hypersalinization of river estuaries in West Africa. Water Resources 35, 367–385.

Mulitza, S., Heslop, D., Pittauerova, D., Fischer, H.W., Meyer, I., Stuut, J.B., Zabel, M., Mollenhauer, G., Collins, J.A., Kuhnert, H., Schulz, M., 2010. Increase in African dust flux at the onset of commercial agriculture in the Sahel region. Nature 466, 226–228.

Myers, N., 2002. Environmental refugees: a growing phenomenon of the 21st century. Philosophical Transactions of the Royal Society 357, 609–613.

Nguetsop, V.F., Servant-Vildary, S., Servant, M., 2004. Late Holocene climatic changes in West Africa, a high resolution diatom record from equatorial Cameroon. Quaternary Science Reviews 23, 591–609.

Nicholson, S.E., 2000. The nature of rainfall variability over Africa on time scales of decades to millenia. Global and Planetary Change 26, 137–158.

Nicholson, S.E., Grist, J.P., 2003. The seasonal evolution of the atmospheric circulation over West Africa and equatorial Africa. Journal of Climate 16, 1013–1030.

Nicklès, M., 1950. Mollusques testacés marins de la côte occidentale d'Afrique. Manuels Ouest-Africains, Vol II. Lechevalier, Paul (Ed.), Paris, 269 pp.

Nizou, J., Hanebuth, T.J.J., Heslop, D., Schwenk, T., Palamenghi, L., Stuut, J.-B., Henrich, R., 2010. The Senegal River mud belt: a high-resolution archive of paleoclimatic change and coastal evolution. Marine Geology 278, 150–164.

Nizou, J., Hanebuth, T.J.J., Vogt, C., 2011. Deciphering signals of late Holocene fluvial and aeolian supply from a shelf sediment depocenter off Senegal (north-west Africa). Journal of Quaternary Science http://dx.doi.org/10.1002/jqs.1467.

Otchere, F.A., Joiris, C.R., Holsbeek, L., 2003. Mercury in the bivalves *Anadara* (*Senilia*) *senilis*, *Perna perna* and *Crassostrea tulipa* from Ghana. The Science of the Total Environment 304, 369–375.
Pagès, J., Citeau, J., 1990. Rainfall and salinity of a Sahelian estuary between 1927 and 1987. Journal of Hydrology 113, 325–341.
Poore, R.Z., Quin, T.M., Verado, S., 2004. Century-scale movement of the Atlantic intertropical convergence zone linked to solar variability. Geophysical Research Letters 31, 4–7.
Reimer, P.J., Baillie, M.G.L., Bard, E., Bayliss, A., Beck, J.W., Bertrand, C., Blackwell, P.G., Buck, C.E., Burr, G., Cutler, K.B., Damon, P.E., Edwards, R.L., Fairbanks, R.G., Friedrich, M., Guilderson, T.P., Hughen, K.A., Kromer, B., McCormac, F.G., Manning, S., Bronk Ramsey, C., Reimer, R.W., Remmele, S., Southon, J.R., Stuiver, M., Talamo, S., Taylor, F.W., Van der Plicht, J., Weyhenmeyer, C.E., 2009. IntCal09 and Marine09 Radiocarbon age calibration curves, 0–50,000 years cal BP. Radiocarbon 51, 1111–1150.
Sadler, J., Carré, M., Azzoug, M., Schauer, A.J., Ledesma, J., Cardenas, F., Chase, B.M., Bentaleb, I., Muller, S.D., Mandeng-Yogo, M., Rohling, E.J., Sachs, J.P., 2012. Reconstructing past upwelling intensity and the seasonal dynamics of primary productivity along the Peruvian coastline from mollusk shell stable isotopes. Geochemistry, Geophysics, Geosystems 13, 1–17.
Salack, S., Muller, B., Gaye, A.T., 2011. Rain-based factors of high agricultural impacts over Senegal. Part I: integration of local to sub-regional trends and variability. Theoretical and Applied Climatology 106, 1–22.
Savenije, H., Pagès, J., 1992. Hypersalinity: a dramatic change in the hydrology of Sahelian estuaries. Journal of Hydrology 135, 157–174.
Schöne, B.R., Fiebig, J., Pfeiffer, M., Gleb, R., Hickson, J., Johnson, A.L.A., Dreyer, W., Oschmann, W., 2005. Climate records from a bivalved Methuselah (*Arctica islandica*, Molluska; Iceland). Palaeogeography, Palaeoclimatology, Palaeoecology 228, 130–148.
Shanahan, T.M., Overpeck, J.T., Anchukaitis, K.J., Beck, J.W., Cole, J.E., Dettman, D.L., Peck, J.A., Scholz, C.A., King, J.W., 2009. Atlantic forcing of persistent drought in West Africa. Science 324, 377–380.
Simier, M., Blanc, L., Aliaume, C., Diouf, P.S., Albaret, J.J., 2004. Spatial and temporal structure of fish assemblages in an "inverse estuary", the Sine Saloum system (Senegal). Estuarine, Coastal and Shelf Science 59, 69–86.
Stager, J.C., Ryves, D., Cumming, B.F., Meeker, L.D., Beer, J., 2005. Solar variability and the levels of Lake Victoria, East Africa, during the last millenium. Journal of Paleolimnology 33, 243–251.
Stige, L.C., Stave, J., Chan, K.S., Ciannelli, L., Pretorelli, N., Glantz, P., Herren, H.R., Stenseth, N.C., 2006. The effect of climate variation on agro-pastoral production in Africa. Proceedings of the National Academy of Sciences of the United States of America 103, 3049–3053.
Stokes, S., Bailey, R.M., Fedoroff, N., Marah, K.E.O., 2004. Optical dating of aeolian dynamism on the West African Sahelian margin. Geomorphology 59, 281–291.
Sultan, B., Baron, C., Dingkuhn, M., Sarr, B., Janicot, S., 2005. Agricultural impacts of large-scale variability of the West African monsoon. Agricultural and Forest Meteorology 128, 93–110.
Thilmans, G., Descamps, C., 1982. Amas et tumulus coquilliers du delta du Saloum. Recherches scientifiques dans les parcs nationaux du Sénégal: Mémoires de l'Institut Fondamental d'Afrique Noire, Dakar, Senegal, pp. 31–50.
Urey, H.C., 1947. The thermodynamic properties of isotopic substances. Journal of the Chemical Society 562–581.
Van Neer, W., Clist, B., 1991. Le site de l'Age de Fer Ancien d'Oveng (Province de l'Estuaire, Gabon), analyse de sa faune et de son importance pour la problématique de l'expansion des locuteurs bantu en Afrique Centrale. Comptes Rendus de l'Académie des Sciences, Paris 312, 105–110.
Verschuren, D., Laird, K.R., Cumming, B.F., 2000. Rainfall and drought in equatorial east Africa during the past 1100 years. Nature 403, 410–414.
Villanueva, M.C.S., 2004. Biodiversité et relation trophiques dans quelques milieux estuariens et lagunaires de l'Afrique de l'Ouest: Adaptations aux pressions environnementales. Ph.D. Thesis, Institut polytechnique de Toulouse, Toulouse, France.
Wanner, H., Solomina, O., Grosjean, M., Ritz, S.P., Jetel, M., 2011. Structure and origin of Holocene cold events. Quaternary Science Reviews 30, 3109–3123.
Wolff, W., Gueye, A., Meijboom, A., Piersma, T., Alassanesall, M.A., 1987. Distribution, biomass, recruitment and productivity of *Anadara senilis* (L.) (Molluska: Bivalvia) on the banc d'Arguin, Mauritania. Netherlands Journal of Sea Research 21, 243–253.
Yamamoto, N., Kitamura, A., Irino, T., Kase, T., Ohashi, S.I., 2010. Climatic and hydrologic variability in the East China Sea during the last 7000 years based on oxygen isotope records of the submarine cavernicolous micro-bivalve *Carditella iejimensis*. Global and Planetary Change 72, 131–140.
Yankson, K., 1982. Gonad maturation and sexuality in the West African bloody cockle, *Anadara senilis* (L.). Journal of Molluscan Studies 48, 294–301.
Zhang, R., Delworth, T.L., 2006. Impact of Atlantic multidecadal oscillations on India/Sahel rainfall and Atlantic hurricanes. Geophysical Research Letters 33 http://dx.doi.org/10.1029/2006GL026267.